



## DEVELOPMENT AND APPLICATION OF A MACHINE VISION SYSTEM FOR MEASUREMENT OF SURFACE ROUGHNESS

D. A. Fadare and A. O. Oni

Mechanical Engineering Department, University of Ibadan, Ibadan, Oyo State, Nigeria

E-Mail: [fadareda@yahoo.com](mailto:fadareda@yahoo.com)

### ABSTRACT

Monitoring of surface roughness is an essential component in planning of machining processes as it affects the surface quality and dimensional accuracy of machined components. In this study, the development and application of a machine vision system suitable for on-line measurement of surface roughness of machined components using artificial neural network (ANN) is described. The system, which was based on digital image processing of the machined surface, consisted of a CCD camera, PC, Microsoft Windows Video Maker, frame grabber, Video to USB cable, digital image processing software (Photoshop, and MATLAB digital image processing toolbox), and two light sources. The images of the machined surface were captured; analyzed and optical roughness features were estimated using the 2-D fast Fourier transform (FFT) algorithm. A multilayer perceptron (MLP) neural network was used to model and predict the optical roughness values. Tool wear index and five features extracted from the surface images were used as input dataset in training and testing the ANN model. The results showed that the ANN predicted optical roughness values were found to be in close agreement with the calculated values ( $R^2$ -value = 0.9529). Thus, indicating that the proposed machine vision system and ANN model are adequate for online monitoring and control of surface roughness in machining environment.

**Keywords:** measurement, surface roughness, machining, image processing, machine vision system, artificial neural network.

### 1. INTRODUCTION

The demand for improved flexibility, productivity, and product quality in modern machining industry has necessitated the need for high-speed, non-contact and on-line monitoring and measurement of surface roughness of machine components. The quality of components produced is of main concern in planning of machining processes as it affects the surface quality and dimensional accuracy of the products [1]. Therefore, critical examination of surface roughness of the components is required as a quality control measure. The conventional method for assessing surface roughness is normally by using stylus type devices, which correlate the vertical displacement of a diamond-tipped stylus to the roughness of the surface under investigation. This method is widely accepted and has been used for many decades in the manufacturing industry [2]. However, this method requires direct physical contact with the surface of the workpiece, which necessitated halting of the machining operations in order to measure the roughness. Hence, this method is time consuming and cumbersome and therefore, not suitable for high-speed and high volume production systems. Another disadvantage of this method is the resolution and the accuracy of the instrument, which depends mainly on the diameter of the tip of the probe of the stylus device.

As a solution to these limitations, other non-contact methods such as atomic force microscopy, phase shifting interferometry, stereo scanning electron microscopy, and laser scanning microscopy has been developed with reasonable success and commercial application of these methods is becoming increasingly popular in manufacturing industry [3-5]. However, all these developed non-contact methods are off-line-based. Hence, they can not be used for on-line and real-time

monitoring and control surface roughness in machining environment.

The application of machine vision system offers better solution in on-line and real-time monitoring surface roughness. Machine vision involves the use of camera, frame grabber, computer system and image processing software to acquire, analyses, monitor, and assess surface roughness parameters. Machine vision systems play an important role in the monitoring and control of automated machining systems. It has generated a great deal of interest in the manufacturing industry [6]. Researchers have shown that the application machine vision has the advantage of being non-contact and has well faster than the contact methods [7]. Using machine vision, it is possible to characterize, evaluate, and analyze the area of the surfaces of machined components.

Several investigations have been carried out using the non-contact optical methods for the assessment surface roughness. These methods are based on statistical analyses of the gray-scale images in the spatial domain [6]. The intensity histograms of the surface image have been utilized to characterize surface roughness and quality [8]. They utilized statistical parameters, derived from the grey level intensity histogram such as the range and the mean value of the distribution and correlated them with the centre line average ( $R_a$ ) value measured with a stylus instrument. Statistical methods such as co-occurrence matrix approach, the amplitude varying rate statistical approach and run length matrix approach have also been used to monitor the texture features of machined surfaces [9]. A 2-D fast Fourier transform (FFT) of the digitized surface image in which the magnitude and frequency information obtained from the FFT are used as measurement parameters of the surface finish has developed by Hoy and Yu [10]. Hisayoshi *et al.* [11] has



reported the estimation of surface roughness using a scanning electron microscope. They showed that the profile of a surface could be obtained by processing back scattered electron signals. Bradley *et al.* [12] employed a fiber optics sensor for surface roughness measurement. In their work, changes in the surface topography are manifested as phase changes of the incident and reflected light on the surface. Kiran *et al.* [13] has reported the application of machine vision system for assessing surface roughness. Priya *et al.* [14] worked on effect of component inclination on the surface roughness using digital image processing. The optical surface finish values ( $G_a$ ) estimated in all such cases using machine vision approach are compared with that obtained using conventional stylus method ( $R_a$ ). An artificial neural network (ANN) was trained and tested to predict the  $R_a$  values using the input obtained from the digital images of inclined surfaces which include optical roughness parameters estimated and angle of inclination of test parts. The results indicated that the surface roughness could be estimated or predicted with a reasonable accuracy using machine vision and ANN model.

Application of ANN in modeling of complex system variables is becoming more popular in many fields of engineering [15]. ANN is essentially an operation linking input data to output data using a particular set of non-linear basic functions. Since ANN modeling is a nonlinear statistical technique, it can be used to solve problems that are not amenable to conventional statistical methods. ANN consists of simple synchronous processing elements which are inspired by biological nervous system. The basic unit in the ANN is the neuron. A neuron is a simple processor, which takes one or more inputs and produces the desired outputs. Each input into the neuron has an associated weight that determines the “intensity” of the input. The processes that a neuron performs are: multiplication of each of the inputs by its respective weight, adding up the resulting numbers for all the inputs

and determination of the output according to the result of this summation and an activation function. Usually neural networks are trained either by either supervised or unsupervised learning algorithms so that a particular set of input produces, as close as possible, a specific set of target outputs [16].

The essence of this work was to develop a machine vision system suitable for on-line, non-contact measurement of surface roughness of machined component using feed-forward multilayer perceptron (MLP) artificial neural network.

## 2. MATERIALS AND METHODS

### 2.1 Description of the machine vision system

The basic components of the machine vision system comprised of a CCD camera (Canon ZR 320 model with a 4.8M pixels resolution) connected with a video to USB cable to a Dell inspiron-6000 PC with 1.5GHz processor and 1.2M bites RAM. Microsoft Windows Video Maker version 5.1 having a 640 by 480 pixels resolution was used for the recording of the digital images and two incandescent spot light bulbs inclined at  $45^\circ$  to the horizontal were used for the illumination of the surface of workpiece material. The frame grabbing function available on the Microsoft Windows Video Maker software was used for capturing different frames (static images) from the recorded video. The captured image of the surface was saved in jpeg format for further analysis. Image processing software which includes: CorelDRAW and digital image processing toolbox for MATLAB were used for the analysis of the captured images. The machined workpiece was clamped using a feature to ensure that the surface was held perpendicularly to the view of the camera. In order to avoid background noise and interference the system was set up in a darkroom. The schematic diagram of the vision system is shown in Figure-1.

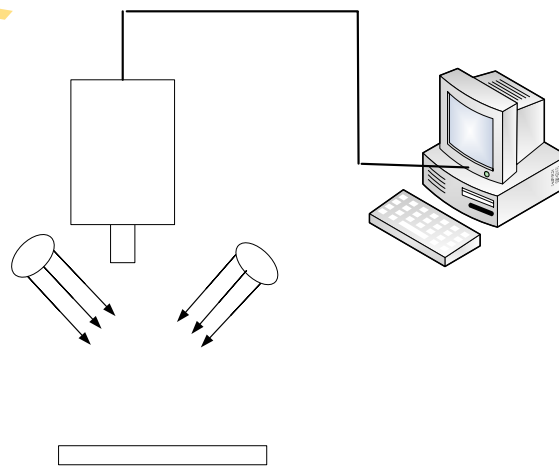


Figure-1. Schematic diagram of the setup of the machine vision system.



## 2.2. Estimation of surface roughness parameters

The most important requirement in roughness assessment using machine vision is to extract the roughness features from the image of the machined surface. In this work, surface roughness features are extracted based on spatial frequency domain using the 2-D fast Fourier transform (FFT) algorithm. Liu and Jernigan [17] and Priya and Ramamoorthy [14] have reported the use of FFT texture features in the spatial frequency domain for characterization surface roughness. In this study, five frequency features, as proposed by Priya and Ramamoorthy [14] and tool wear index (TWI) [6] were used to characterise the surface roughness of the machined workpiece.

### 2.3 The fast Fourier Transform (FFT) analysis

Let  $f(m, n)$  be the grey level of a pixel at  $(m, n)$  in the original image of size  $N$  by  $N$  pixels centered on the origin. The discrete 2D Fourier transform of  $f(m, n)$  is given as [14]

$$F(u, v) = \sum_{m=-\infty}^{\infty} \sum_{n=-\infty}^{\infty} f(m, n) e^{-j\omega_1 m} e^{-j\omega_2 n} \quad (1)$$

Where  $\omega_1$  and  $\omega_2$  are frequency variables and  $F(u, v)$  is the frequency domains representation of  $f(m, n)$ .

$F(u, v)$  is a complex-valued function that is periodic both in  $u$  and  $v$ , with period  $2\pi$ . Because of the periodicity, usually only the range  $-\pi \leq u, v \leq \pi$  is displaced. The Fourier transform is generally complex, i.e.

$$F(u, v) = R(u, v) + jI(u, v) \quad (2)$$

Where  $R(u, v)$  and  $I(u, v)$  are the real and imaginary components of  $F(u, v)$ , respectively. The power spectrum  $P(u, v)$  of  $f(u, v)$  is defined by

$$P(u, v) = |F(u, v)|^2 = R^2(u, v) + I^2(u, v) \quad (3)$$

The normalized power spectrum, which has the characteristics of a probability distribution, is defined as

$$p(u, v) = \frac{P(u, v)}{\sum_{(u, v) \neq (0, 0)} P(u, v)} \quad (4)$$

Where  $P(u, v)$  is the power spectrum of the image  $I(m, n)$ .

#### 2.3.1 Major peak frequency (F1)

The major peak frequency is defined as [14]

$$F1 = (u^2 + v^2)^{1/2} \quad (5)$$

Where  $u$  and  $v$  are the frequency coordinates of the maximum peak of the power spectrum, i.e.

$$p(u, v) = \max[p(u, v) \forall (u, v) \neq (0, 0)] \quad (6)$$

Feature  $F_1$  is the distance of the major peak  $(u_1, v_1)$  from the origin  $(0, 0)$  in the frequency plane.

#### 2.3.2 Principal component magnitude squared (F2)

The principal component magnitude squared is defined as [14]

$$F2 = \lambda_1 \quad (7)$$

Where  $\lambda_1$  is the maximum eigenvalue of the covariance matrix of  $p(u, v)$ . The covariance matrix  $M$  is given by

$$M = \begin{bmatrix} \text{var}(u^2) & \text{var}(uv) \\ \text{var}(vu) & \text{var}(v^2) \end{bmatrix} \quad (8)$$

For which

$$\text{var}(u^2) = \sum_{(u, v) \neq (0, 0)} u^2 p(u, v), \quad (9)$$

$$\text{var}(v^2) = \sum_{(u, v) \neq (0, 0)} v^2 p(u, v), \quad (10)$$

$$\text{var}(uv) = \text{var}(vu) = \sum_{(u, v) \neq (0, 0)} uv p(u, v) \quad (11)$$

Feature  $F_2$  indicates the variance of components along the principal axis in the frequency plane.

#### 2.3.3 Average power spectrum (F3)

The average value of power spectrum is defined as [14]

$$F3 = \sum P(u, v) / S \quad (12)$$

and  $(u, v) \neq (0, 0)$

Where  $S = N^2 - 1$  for a surface image of size  $N \times N$ .

#### 2.3.4 Central power spectrum percentage (F4)

The central power spectrum percentage is defined as [14]

$$F4 = \frac{P(0, 0)}{\sum_u \sum_v P(u, v)} \times 100\% \quad (13)$$

The frequency component at the origin of the frequency plane has the maximum power spectrum.

#### 2.3.5 Ratio of major axis to minor axis (F5)

The ratio of major axis to minor axis is defined as [14]

$$F5 = (\lambda_1 / \lambda_2)^{1/2} \quad (14)$$

Where  $\lambda_1$  and  $\lambda_2$  are the maximum and minimum eigenvalues of the covariance matrix of  $P(u, v)$ .

#### 2.3.6 Tool wear index (TWI)

A tool wear index extracted from digital image processing of tool wear images is defined as [6]

$$TWI = \frac{[(\sum (Aw_f)^2 + (\sum (Aw_n)^2)]^{0.5}}{[(Em_f)^2 + (Em_n)^2]} \quad (15)$$



Where  $Aw_f$  is the wear area on the flank,  $Aw_n$  is wear area on the nose,  $Em_f$  is the equivalent diameter of flank wear, and  $Em_n$  is the equivalent diameter of nose wear.

### 2.3.7 Optical roughness

The optical roughness value ( $G_a$ ) defined as the arithmetic average of grey level intensity values [14]. It was estimated as

$$G_a = \frac{1}{n} \sum_{i=1}^n |g_i| \quad (16)$$

Where  $g_i$  is the difference between the grey level intensity of individual pixels in the surface image and the mean grey value of all the pixels under consideration.

The five frequency features (F1, F2, F3, F4, and F5) and the tool wear feature (TWI) were used as input parameters for the training and testing of the neural network, while the optical roughness was used as output parameter.

## 2.4 Development of the neural network model

### 2.4.1 Design of the ANN model

Neural Network Toolbox for MATLAB® was used to design the neural network. The basic steps involved in designing the network were: Generation of data; Pre-processing of data; Design of the neural network elements; Training and testing of the neural network; Simulation and prediction with the neural networks; and Analysis and post-processing of predicted result.

### 2.4.2 Generation of dataset

In order to generate input/output dataset for training and testing of the network, series of turning operations were carried out and the surface of machined workpiece was captured and analysed using the proposed machine vision system. The turning operations were conducted on Harrison M300 lathe powered with a 2.2 kW, 3-phase, 1500rpm induction motor. The workpiece material used for the turning operation was NST 37.2 steel bar with 25 mm diameter obtained from the Delta Steel Company (DSC), Ovia Aladja, Nigeria. SANDVIC Coromant® cutting inserts with ISO designation SNMA 120408 were used for turning operation. The cutting geometry of the insert was: approach angle,  $75^\circ$ , side rake angle,  $-6^\circ$ , back rake angle,  $-6^\circ$  and clearance angle,  $6^\circ$ . The cutting parameters used were: feed rate ( $f$ ) = 1.0, 1.8, 2.2 mm/rev; cutting speed ( $v$ ) = 20.42, 29.06, and 42.42 mm/s; and depth of cut ( $a$ ) = 0.2, 0.4, 0.8 mm. Eight passes of 50 mm length of cut were taken for the different conditions of the cutting parameters. A total of 27 cutting experiments were conducted. All the cutting operations were conducted without the application of coolant. The machined surface of the workpiece was captured and analysed after each pass for the different cutting

conditions. The frequency features (F1, F2, F3, F4, and F5), optical roughness and the tool wear feature (TWI) were extracted from the captured image of the machined surface and the tool insert.

### 2.4.3 Pre-processing of data

The input/output dataset were normalized to range between 0 and 1 using the 'premnmx' function. The dataset was then portioned randomly into two subsets: training dataset (75%), and testing dataset (25%).

### 2.4.4 Design of the neural network elements

Feed-forward multilayer perceptron (MLP) neural network with 3 layers was designed, trained and tested. There were six neurons in the input layer, five in the hidden layer, while there was one neuron in the output layer. The structure of the neural network is shown in Figure-2.

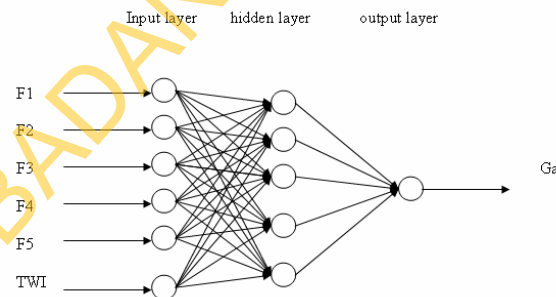


Figure-2. The model of feed-forward multilayer ANN used to predict optical roughness.

### 2.4.5 Training of the neural network

The Levenberg-Marquardt (*trainlm*) [18], back-propagation training algorithm, commonly used because of its fast convergence and accuracy was used for training the network. The tan-sigmoid transfer function 'tansig' was used in the hidden layer, while linear transfer function 'purelin' was used in the output layer. The 'purelin' transfer function was used in the output layer.

### 2.4.6 Testing of the ANN model

The mean square error (MSE) between the predicted and the desired outputs was used as the performance function during the training phase. The training was terminated when the threshold of MSE = 0.001 or when the number of iterations equal to 1000 is attained. The predictive performance accuracy of the network was determined based on the coefficient of determination ( $R^2$ -value) between the predicted and the actual values of optical roughness of the machined surface.

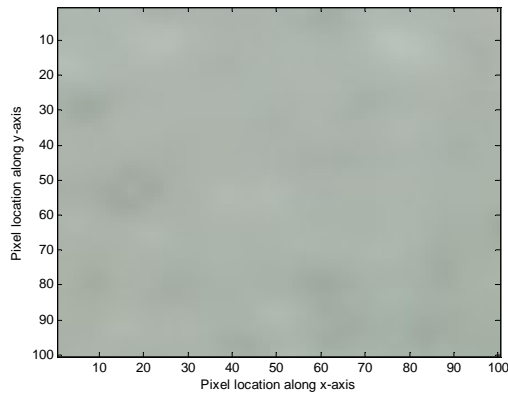
## 3. RESULTS AND DISCUSSIONS

Typical gray-scale images, and 3-D plots of the pixel intensity of the machined surface obtained after machining with cutting parameters ( $v = 20.42$  mm/s,  $f = 0.2$  mm/rev,  $a = 1.0$  mm) for passes 1, 3, and 4 for arc

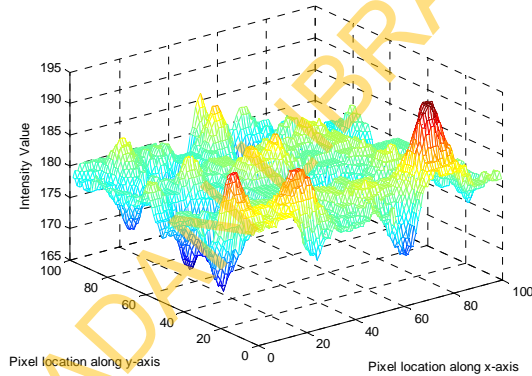


shown in Figure-3. It can be seen, that as the number of pass increased the surface get rougher due to increase in tool wear. Hence, the pixel intensity of the image of machined surface increased with number of pass. The comparison between the ANN predicted optical roughness and the actual values for the test dataset is shown Figure-4. The result showed that the ANN model was able to model and predicts the optical roughness with a high accuracy with a coefficient of determination of 95.29%.

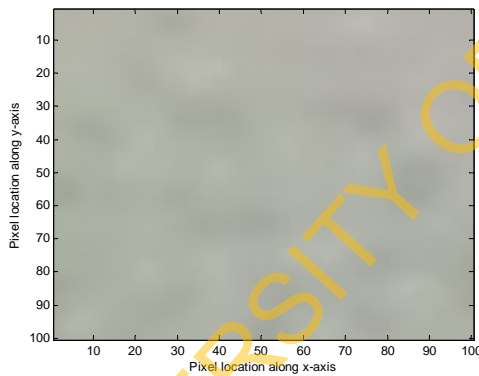
The extracted roughness features: F1, F2, F3, F4, and F5, TWI, actual optical roughness and the ANN predicted optical roughness for different passes at the cutting condition ( $v = 20.42$  mm/s,  $f = 0.2$  mm/rev,  $a = 1.0$  mm) are presented in Table-1. The absolute error between the actual and ANN predicted optical roughness for this cutting condition was less than 0.05. Thus, indicating the high accuracy of the proposed machine vision system and the ANN model for on-line monitoring of surface roughness of machined components.



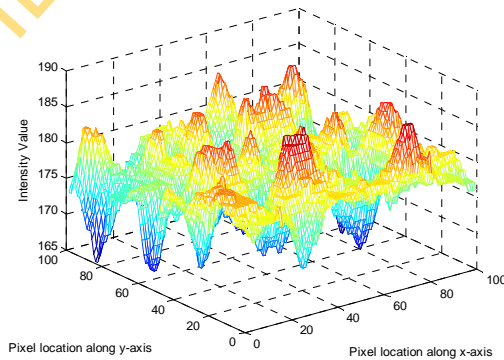
(a) Pass 1



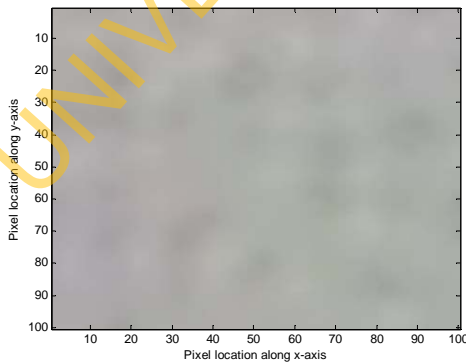
(b) Pass 1



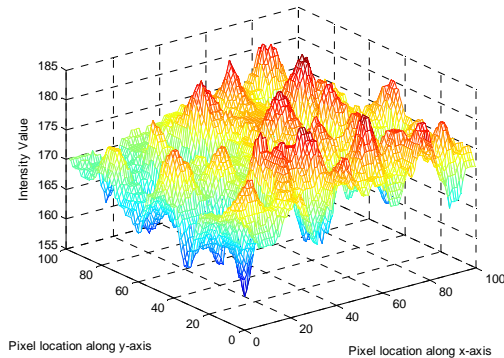
(a) Pass 3



(b) Pass 3



(a) Pass 4



(b) Pass 4

**Figure-3.** Typical gray scale image (a), and pixel intensity plot (b) of the machined surface obtained at different passes for cutting parameters ( $v = 20.42$  mm/s,  $f = 0.2$  mm/rev,  $a = 1.0$  mm).

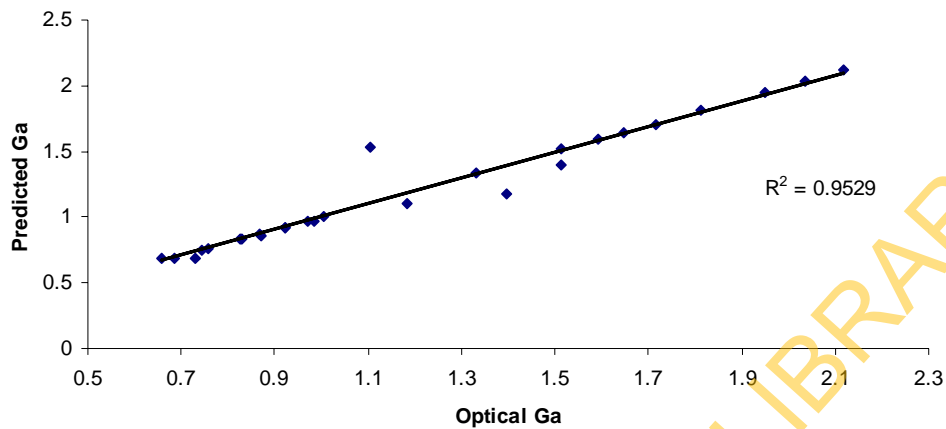


**Figure-4.** Comparison between ANN predicted and actual values of optical surface roughness for the test dataset.

**Table-1.** Calculated roughness parameters, tool wear Index (TWI), actual optical surface roughness ( $G_a$ ) and ANN predicted values for different passes at cutting condition ( $v = 20.42$ ,  $f = 0.2$ ,  $a = 0.1$ mm).

| No. of pass | F1      | F2      | F3 x10 <sup>6</sup> | F4      | F5     | TWI     | Actual optical ( $G_a$ ) | ANN predicted ( $G_a$ ) | Absolute error |
|-------------|---------|---------|---------------------|---------|--------|---------|--------------------------|-------------------------|----------------|
| 1           | 43.705  | 2843.67 | 2.62                | 95.0604 | 3.9852 | 0.06959 | 0.658                    | 0.689                   | 0.0311         |
| 2           | 40.14   | 2441.99 | 2.75                | 97.6947 | 3.4044 | 0.11699 | 0.684                    | 0.684                   | 0.0000         |
| 3           | 43.7786 | 2851.00 | 2.46                | 95.3156 | 4.0145 | 0.33355 | 0.731                    | 0.691                   | 0.0403         |
| 4           | 53.581  | 2799.62 | 3.07                | 93.5983 | 3.8420 | 1.54709 | 0.759                    | 0.760                   | 0.0010         |
| 5           | 69.8231 | 2834.19 | 3.52                | 93.3086 | 3.5610 | 1.89721 | 0.826                    | 0.838                   | 0.0120         |
| 6           | 38.4472 | 3243.59 | 4.47                | 93.486  | 3.2672 | 3.18722 | 0.831                    | 0.835                   | 0.0040         |
| 7           | 57.1899 | 3087.14 | 4.04                | 91.9414 | 3.4885 | 4.55688 | 0.872                    | 0.853                   | 0.0190         |
| 8           | 65.3817 | 2472.10 | 3.91                | 93.6729 | 2.8376 | 8.85766 | 0.924                    | 0.924                   | 0.0000         |

### 3.1 Design of graphical user interface (GUI)

A graphical user interface (GUI), was designed using the GUI toolbox for MATLAB<sup>®</sup> for ease application of the vision system and the ANN model in analysing surface roughness of machined components. The GUI was divided into parts: input, and output section. The input section consists of a field text where the file name of the captured surface image to be analysed is entered. On pressing the 'acquire image' button, the captured surface image is loaded to the graphic window and the file name of the image is also displayed on the window. The frequency coordinates of the maximum peak of the power spectrum U and V (Eqn. 5) of the image is entered and the FFT of the image is executed by pressing the 'FFT MSEH' button. The roughness features F1 to F7, actual optical roughness and ANN predicted roughness are estimated by pressing the 'analyse' button. The values of the roughness features F1 to F5, and the ANN predicted optical roughness are displayed in the different designated

numeric field box, while the corresponding degree of roughness F6 and F7 of the surface are displayed in the different designated numeric field box.

An illustrative example of the application of the GUI for the analysis of surface roughness for cutting parameter ( $v = 20.42$  mm/s,  $f = 0.2$  mm/rev,  $a = 1.8$  mm) is shown in Figure-4. The captured surface image of the workpiece after pass three (3) was saved with the file name 'ga11. ipg'. For this image, the extracted features were: F1 (44.5997), F2 (2842.678), F3 (2.61785), F4 (95.0604), F5 (3.98523), F6 (709745), F7 (19.2445), and ANN predicted optical roughness,  $G_a$  (0.657669).

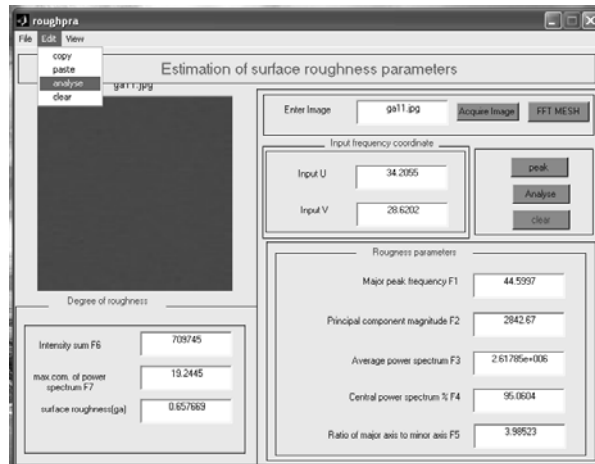


**Figure-4.** GUI developed for measurement of surface roughness.

#### 4. CONCLUSIONS

A machine vision system suitable for on-line, non-contact measurement of surface roughness of machined component using feed-forward multilayer perceptron (MLP) artificial neural network has been developed and applied for measurement of surface roughness of NST 37.2 steel workpiece machined with a SANDVIC Coromant cutting inserts with ISO designation SNMA 120408. The study clearly demonstrated the feasibility of using machine vision and ANN model in on-line monitoring and measurement of surface roughness of machined surfaces. The machined surface roughness image was captured and transformed using 2-D fast Fourier transform (FFT) algorithm. Five roughness features were extracted from the image and actual optical roughness was estimated. ANN model has been used to model and predict the optical roughness using the tool wear index (TWI) and five optical features extracted from the images were used as inputs to the network. The ANN predicted roughness values were found to be in close agreement with the actual optical roughness with  $R^2$ -value = 0.9529. The proposed machine vision and ANN model can be used with acceptable accuracy for on-line monitoring of surface roughness of machined components.

#### REFERENCES

- [1] K. Yongjin, G.W. Fischer. 2003. A novel approach to quantifying tool wear and tool life measurement for optimal tool management, *International Journal of Machine Tools and Manufacture*. 43(4): 359-368.
- [2] T.R. Thomas. 1999. *Rough surface*. Imperial College Press, London.
- [3] S.N. Magonov, M.N. Whangbo. 1996. *Surface analysis with STM and AFM*. Springer-Verlag. Berlin.
- [4] B. Bhushan, J.C. Wyant, C.L. Kaliopoulos. 1985. Measurement of surface topography of magnetic tapes by Mirau interferometry. *Appl. Opt.* 28: 1489-1497.
- [5] P. Podsiadio, G.W. Stachowiak. 1997. Characterization of surface topography of wear particles with SEM stereoscopy. *Wear* 206: 39-52.
- [6] A.O Oni. 2007. Development of a machine vision system for measurement of tool wear and surface roughness. Unpublished M.Sc desertation, University of Ibadan, Nigeria.
- [7] G.A. Al-Kindi, R.M. Baul, K.F. Gill. 1992. An application of machine vision in the automated inspection of engineering surfaces, *International Journal of Production Research* 30(2): 241-253.
- [8] F. Luk, V. Hyunh, and W. North. 1989. Measurement of surface roughness by a machine vision system, *Journal of Physics E Scientific Instruments* 22: 977-980.
- [9] R.K. Venkata, B. Ramamoorthy. 1996. Statistical methods to compare the texture features of machine surfaces, *Pattern Recognition*. 29(9): 1447-1459.
- [10] D.E.P. Hoy, F. Yu. 1991. Surface quality assessment using computer vision methods, *Journal of Materials Processing Technology*. 28 (1-2): 265-274.
- [11] S. Hisyoshi, O-H. Masanori. 1982. Surface roughness measurement by scanning electron microscope, *Annals of CIRP* 31:457-462.
- [12] C. Bradley, J. Bohlmann, S. Kurada. 1998. A fiber optic sensor for surface roughness measurement. *Journal of Manufacturing Science and Engineering* 120: 359-367.
- [13] M.B. Kiran, B. Ramamoorthy, B. Radhakrishnan. 1998. Evaluation of surface roughness by vision system. *International Journal of machine Tools and Manufacture*. 38(5-6): 685-690.
- [14] P. Priya, B. Ramamoorthy. 2007. The influence of component inclination on surface finish evaluation using digital image processing, *International Journal of Machine tools and manufacture*. 47(3-4): 570-579.
- [15] S. Malinov, W. Sha, J.J. McKeown. 2001. Modeling the correlation between process parameters and properties in titanium alloy using artificial neural network. *Computational Material Science*. 21: 375-394.
- [16] M.S. Alajmi, S. E. Oraby, I.I. Esat. 2005. Neutral network models on the prediction of tool wear in turning process: A comparison study. *Proceeding of*



---

www.arpnjournals.com

the 45<sup>th</sup> Conference on Artificial Intelligence and Applications.

- [17]S. Liu, M.E. Jernigan. 1990. Texture analysis and discrimination in additive noise. Computer Vision, Graphics, and Image Processing. 49(1): 52-67.
- [18]H. Demuth, M. Baale. 2000. Neural network toolbox manual. Mathworks Inc. USA.

UNIVERSITY OF IBADAN LIBRARY